Desalination and Water Treatment
www.deswater.com

doi: 10.1080/19443994.2015.1112980

57 (2016) 20210–20218
September

Taylor & Francis
Taylor & Francis Group

Modeling seawater reverse osmosis system under degradation conditions of membrane performance: assessment of isobaric energy recovery devices and feed pressure control benefits

Kwanho Jeong[a], Young Geun Lee[b], Seo Jin Ki[a], Joon Ha Kim[a,*]

[a]*School of Environmental Science and Engineering, Gwangju Institute of Science and Technology (GIST), Gwangju 500-712, Korea, Tel. +82 62 7153277; Fax: +82 62 7152434; email: joonkim@gist.ac.kr (J.H. Kim)*
[b]*Water Business Group, Doosan Heavy Industries and Construction Co., Ltd, Gyeongsangnamdo 642-792, Korea*

Received 1 September 2015; Accepted 9 October 2015

ABSTRACT

A transient model of seawater reverse osmosis (SWRO) system enables systematic assessment of membrane performance in response to changes in time-series parameters, operating conditions, or ancillary equipment. In this study, we describe the effects of energy recovery device (ERD) and feed pressure control on the SWRO plant in terms of energy consumption (reduced) and water quantity (increased) using a numerical model at pilot scale. In the simulation, two types of isobaric ERD, i.e. pressure exchanger (PX) and dual work exchanger energy recovery (DWEER), were used to quantify changes of the mass flow rates of inflow and outflow in the system. Also, temporal variation in the raw feedwater quality was addressed in the model with adaptive feed pressure control to maintain the amount of produced water under fouled membrane conditions. Results showed that the observed recovery and rejection rates in the pilot-scale plant had an excellent agreement with their predicted values under different seawater feed concentrations varied over a year (NSE = 0.9990 and 0.9987, respectively). Both PX and DWEER were found to affect the concentration and stream of influent directed to the reverse osmosis module, in which PX showed slightly higher recovery rate than DWEER that had the volumetric flow loss of the pressurized feed. While water quality and quantity of the permeate declined progressively in non-steady state simulation of membrane fouling, increasing the feed pressure linearly improved the performance of the pilot plant, higher recovery rate and lower energy consumption than a constant pressure mode. Therefore, this study demonstrates that the dynamic simulation model for the SWRO system not only describes deterioration of membrane performance at the pilot scale, but also can be used to search alternative devices and operation modes that achieve water quality and quantity targets with efficient energy use.

Keywords: Seawater reverse osmosis; Energy recovery device; Feed pressure control; Membrane fouling; Energy consumption

*Corresponding author.

1. Introduction

Reverse osmosis (RO) purifying water from a pressure-driven membrane process now becomes dominant in desalination markets around the world due to low-energy consumption to produce fresh water [1]. In the RO process, the permeate (i.e. the decontaminated water) and the concentrate (i.e. the liquid retaining large particles or ions) are separated across a semipermeable membrane using an external pressure that exceeds the natural flow from high to low water potentials. Separation efficiency, unlike other membrane technologies, was known to be determined by various operational parameters such as raw seawater quality (or solute concentration), influent pressure, and water flux rate (as a function of membrane properties). Membrane fouling occurred as foulants were strongly accumulated on a membrane surface or inside the membrane, deteriorating membrane performance such as increases in salt passage and energy consumption as well as flux decline. Membrane fouling was difficult to avoid in the long run although cleaning fouled membranes using physical and chemical methods was found to mitigate the fouling rate effectively [2]. Therefore, optimizing operational conditions in response to temporal degradation of membrane performance is needed to constantly maintain the quantity and quality of produced water during long-term operation in a seawater reverse osmosis (SWRO) plant.

The introduction of energy recovery device (ERD) enables us to reduce energy consumption in the SWRO plant by transferring high pressure of the concentrate to the feedwater [3,4]. The ERD can be divided into two distinct types, a centrifugal ERD and an isobaric ERD, depending on their energy transfer principles [5]. The centrifugal ERD converts hydraulic energy of high-pressure fluid into mechanical energy of turbines or pumps [6], whereas the isobaric ERD directly exchanges the hydraulic energy between the low-pressure feed and the high-pressure concentrate, thereby lowering energy loss [7,8]. Examples of the centrifugal ERD commercially available are Pelton impulse turbine and hydraulic turbocharger. Pressure exchanger (PX) and dual work exchanger energy recovery (DWEER) belong to the isobaric ERD, for example. Despite high efficiency of pressure transfer (>95%), the isobaric ERD, however, had several inherent problems such as mixing, leakage, overflush, and differential head [4]. Among them, the mixing and overflush, occurred when the feed and the concentrate were interchanged, were found to generally exhibit dominant effects on the SWRO process by increasing salt concentration of the feedwater and decreasing its volumetric flow rate [6,9]. However, as their relative importance varies from one system to another, the benefits of each type of ERD should be carefully evaluated by experimental or simulation studies under various operating conditions in the SWRO plant.

The current programs typically used for simulation of the full-scale SWRO system are not able to describe a dynamic behavior of membrane performance due to the steady state assumption of temporal processes. This indicates that they do not correctly capture the progressive development of membrane fouling as well as assess the performance of the SWRO plant in response to changes in operating conditions and additional facilities supported. In this study, we develop, therefore, a numerical model to investigate temporal changes in the mass flow rates (i.e. the quantity and quality of produced water) in the pilot-scale SWRO plant. Using this model, we specifically (1) identify the effect of the isobaric ERD (i.e. PX and DWEER) on energy consumption, (2) characterize membrane fouling in response to changes in the raw feedwater quality, and (3) address the benefits of increasing the feed pressure under degradation conditions of membrane performance. From this study, we expect that the simulation study is useful not only for improving operation and maintenance activities, but also for optimizing energy consumption and costs for the SWRO plant.

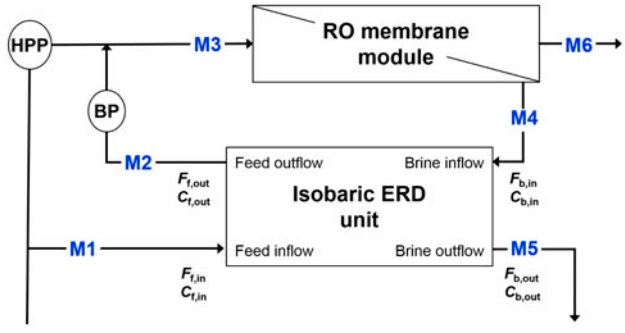

Fig. 1. Schematic diagram of the mass flow rates (i.e. water flow F and solute C) at different monitoring points (M1, M2, M3, M4, M5, and M6) in the SWRO system mounting with isobaric ERDs. HPP and BP indicate high pressure (that increases the feed pressure of inflow to the RO membrane module) and booster pumps (that increases the feed pressure of outflow from the isobaric ERDs), respectively. Subscripts f and b denote the feed and brine (or concentrate), respectively.

2. A pilot-scale model for SWRO system

2.1. Description of main processes and numerical procedures

Fig. 1 illustrates a schematic diagram in the pilot-scale SWRO plant to simulate the mass flow rates (i.e. a water and solute) in the RO membrane module and isobaric ERD unit. In the system, the combined feed stream (at the point M3) from the raw seawater and isobaric ERD passed through the RO membrane module, which produced the permeate (at the point M6) and concentrated brine. The feed in low pressure (at the point M1) met the brine in high pressure (at the point M4) in the isobaric ERD, where the hydraulic pressure (or energy) as well as the water and solute mass were exchanged each other. The isobaric ERD then discharged both the feed increased slightly in salinity level (at the point M2) and the brine declined highly in pressure level (at the point M5). Note that the RO membrane module of the pilot scale, in fact, consists of two subelements; each has a capacity of producing 7.4 m^3 of water in a day with 8% recovery rate.

Based on the configuration of the SWRO plant, we developed the transient simulation model to assess the effects of the isobaric ERD and feed pressure control on membrane performance under temporal evolution of membrane fouling. Fig. 2 shows simulation steps to compute the mass flow rates in the SWRO plant using three governing equations, the mass balance equation for the ERD unit as well as the transport and fouling equations for the RO module. Conserving the water and solute mass, the simulation model updates the resistance and permeate flux from the fouling and transport equations at one-minute intervals, respectively. Changes in the brine and feed mass flow rates are then provided to the mass balance and transport equations, respectively, to recalculate the water and solute mass at the next time step. Iterative calculation of water and solute transport for individual equations is stopped after one-year simulation period. Note that hourly seawater data are provided during the simulation to reflect the raw feedwater quality variation for the SWRO plant at the pilot scale. Time-series monitoring data recorded around Young Island at Busan in Korea for 2010 were obtained from the Marine Environment Information System in Korea. The hourly records of salt concentration and temperature were further disaggregated into one-minute data using a linear interpolation method to match the simulation time step. The governing equations employed for the pilot-scale model are described in detail in the following sections.

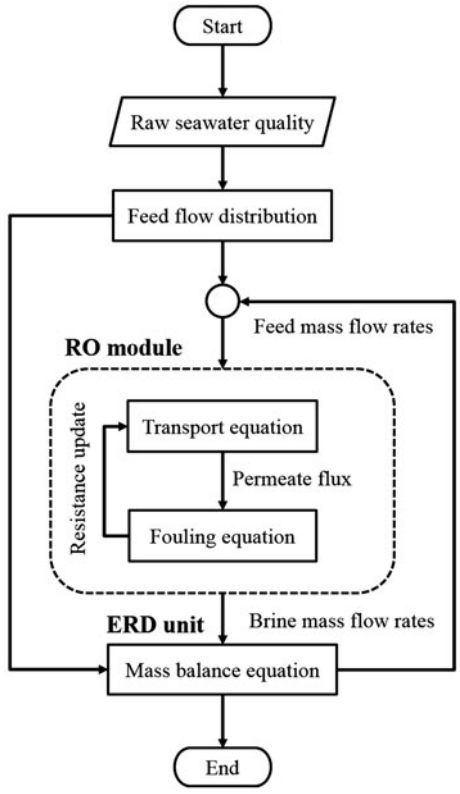

Fig. 2. Numerical simulation procedures to estimate the mass flow rates in the given SWRO system. During the simulation, the mass flow rates are designed to be iteratively updated by three governing equations, the RO membrane transport, fouling, and isobaric ERDs models. Note that time series of marine monitoring data around Young Island at Busan in Korea are used to reflect seasonal variations in the raw feedwater quality to the SWRO system.

2.2. RO membrane module

The RO membrane transport model developed by Kedem and Katchalsky [10,11] was used to assess the membrane performance of the SWRO plant under various operating conditions. The transport equation used in this study is well known as the irreversible thermodynamic model, which allows us to estimate the water and salt fluxes of the RO membrane. In the model, water flux across the membrane J_w is described by the Darcy's law that is derived from the difference between the transmembrane pressure and the osmotic pressure, as shown in Eq. (1). Salt flux J_s is quantified by two different transport mechanisms (see Eq. (2)), the solute concentration gradient (i.e. the Fick's laws of diffusion) and the coupling transport of a solute and a solvent (i.e. convection) [12].

$$J_w = L_p(\Delta p - \sigma\Delta\pi) \quad (1)$$

$$J_s = P_m\Delta c + (1-\sigma)J_w\bar{c} \quad (2)$$

where L_p and P_m are the pure water permeability and salt permeability of the membrane, respectively. The Staverman reflection coefficient, σ, determines the degree of coupling between water and solute fluxes. The transmembrane hydraulic pressure, osmotic pressure, and difference in salt concentration across the membrane active layer are represented by Δp ($=p_f - p_p$), $\Delta\pi$, and Δc, respectively. The feed and permeate pressures are indicated by p_f and p_p, respectively, and the arithmetic average of salt concentration is denoted as $\bar{c}$.

The modified van't Hoff equation [13] is employed to calculate the transmembrane osmotic pressure, such that

$$\Delta\pi = \frac{N_{ion}R_gT\Delta c}{M_w} \quad (3)$$

$$\text{where } \Delta c = c_w - c_p \quad (4)$$

where N_{ion}, R_g, T, and M_w indicate the number of ions in the feed solution, universal gas constant, absolute temperature, and molecular weight of the salt, respectively. c_w and c_p are the membrane wall and permeate concentrations, respectively. Note that in Eq. (4), we use c_w instead of the membrane feed concentration c_f to avoid the underestimation of the transmembrane osmotic pressure resulting from a concentration polarization (CP) occurred around the membrane surface. Due to very high salt rejection rates of the membranes typically used in the SWRO process (reaching over 99%), c_p is often neglected in estimating the difference in salt concentraiton across the membrane. The CP representing the ratio from c_w to c_{bulk} can be described using the film theory model [14]. Assuming the complete rejection of the solute by the membrane [14], the membrane wall concentration of the salt c_w is then calculated as:

$$c_w = c_{bulk}\exp\left(\frac{J_w}{k}\right) \quad (5)$$

where c_{bulk} denotes the bulk salt concentration of the feed channel. k represents the mass transfer coefficient which can be estimated by the Sherwood correlation as follows [14]:

$$\text{Sh} = kd_h/D = 0.04\,\text{Re}^{0.75}\,\text{Sc}^{0.33} \quad (6)$$

where Sh, Re ($=\rho d_h u/\mu$), and Sc ($=\nu/D$) indicate the (dimensionless) Sherwood, Reynolds, and Schmidt numbers, respectively. u and d_h are the velocity and hydraulic diameter of the flow channel, respetively, whereas D is the diffusion coefficient of the solute. The parameters ρ, μ, and ν represent the density, dynamic viscosity, and kinematic viscosity of water, respetively. Note that the Sherwood correlation is valid when describing the turbulent cross flow in a rectangular channel such as a spacer-filled channel [15].

Previous study [16] showed that the temporal degradation of membrane performance was successfully described by the total membrane resistance (R_m), which provided an additional hydraulic resistance of the fouling layer over time with the intrinsic resistnace of a clean membrane (R_{m0}).

$$R_m(x,\ t) = R_{m0} + k_{fp}\int_0^t v_w(x,\ \tau)\,d\tau \quad (7)$$

where k_{fp} is the coefficient that represents the fouling potential of the feedwater and v_w refers to the permeate velocity. The parameters x, t, and τ represent the horizontal location in the membrane channel, time step, and dummy variable used for integration, respectively.

2.3. Isobaric ERD unit

The isobaric ERD unit consists of two inflows and outflows (see Fig. 1). Based on the principle of a mass balance, we develop the diffferential equation for the overall (i.e. water and solute) mass flow rate, which is expressed as:

$$\frac{dm_{f,out}}{dt} = F_{f,in} + F_{b,in} - F_{b,out} \quad (8)$$

$$\text{where } F_{b,out} = F_{b,in} + \text{OV}\cdot F_{f,in} \quad (9)$$

where $m_{f,out}$ refers to the overall mass of the pressurized feedwater. $F_{f,in}$ and $F_{b,in}$ denote the overall mass flow rates of the influents for the feed and brine, respectively, whereas $F_{b,out}$ represents that of the effluent for the brine. The parameter OV indicates the overflush ratio which is determined by the difference between $F_{f,in}$ and $F_{f,out}$.

In addition, the diffferential equation for the solute can be written as:

$$\frac{dm_{b,out}}{dt} = F_{f,in}C_{f,in} + F_{b,in}C_{b,in} - F_{f,out}C_{f,out} \quad (10)$$

$$\text{where } C_{f,out} = M\left(C_{b,in} - C_{f,in}\right) + C_{f,in} \quad (11)$$

where $m_{b,out}$ is the solute mass of the depressurized brine. While $C_{b,in}$ and $C_{f,in}$ indicate the concentrations of the influents for the high-pressure brine and low-pressure feed, respectively, $C_{f,out}$ represents that of the effluent for the pressurized feed. M denotes the volumetric mixing ratio between the feed and brine streams caused by the hydraulic energy transfer in the ERD unit. Using this ratio, we are able to estimate the increased salinity of the feed stream at the monitoring point M2. Note that specific energy consumption (SEC) for different operation scenarios (i.e. the feed pressure control and ERD) in the SWRO plant was estimated based on [17].

3. Results and discussion

3.1. Model validation

Fig. 3(a) and (b) exhibit the temporal profiles of the raw feedwater quality (i.e. the salt concentration and temperature in seawater, respectively) for 2010 which are used as input for the pilot-scale model. As shown in both figures, there was a great variation in the raw feedwater quality in a year, implying that this should be addressed in the simulation to correctly describe the degradation of membrane performance over time. On average, while the salt concentration recorded 32,921 and 29,175 mg/L for winter and summer seasons, respectively, their corresponding temperature values were 12.5 (for a winter season) and 21.5℃ (for a summer season).

The results of model validation with respect to the permeate recovery rate and salt rejection rate are illustrated in Fig. 4(a) and (b), respectively. The simulation was run separately under various feed salt concentrations that were equivalent to those measured in the pilot-scale plant. By increasing the feed salt concentration c_{bulk} at 2,000 mg/L intervals in the range of 28,000 to 36,000 mg/L, the model was evaluated under specified operating conditions: u (the velocity of the flow channel) = 9.65×10^{-2} m/s (=30 L/min), p_f (the feed pressure) = 65 bar, and T (the feed temperature) = 293.15 K. From the figures, the predicted values for the recovery rate and salt rejection rate were in excellent agreement with the observed data (NSE = 0.9987–0.9990), indicating the model successfully described the dynamic behavior of water and solute movement in the SWRO plant at the pilot scale.

3.2. The impacts of isobaric ERD

The volumetric mixing and overflush of the isobaric ERD have the negative impacts on the SWRO process by either reducing the feed flow rate or increasing its salinity level that are provided for the RO membrane module (see Fig. 1). Based on the previous study [4], PX was assumed to have the properties of the 6% mixing rate and no contribution of the overflush during the pressure transfer, whereas DWEER was characterized by the 1.5% mixing rate and 3% overflush. Table 1 shows the simulation results of the pilot-scale plant using the assumed

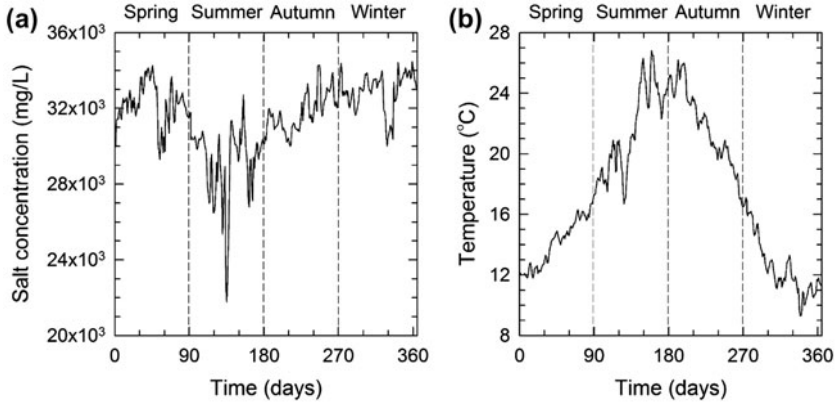

Fig. 3. Seasonal variations of (a) NaCl concentration and (b) temperature in seawater monitored at Young Island at Busan in Korea for 2010. The spring season includes March, April, and May, and the other seasons consist of the following three months in series for each.

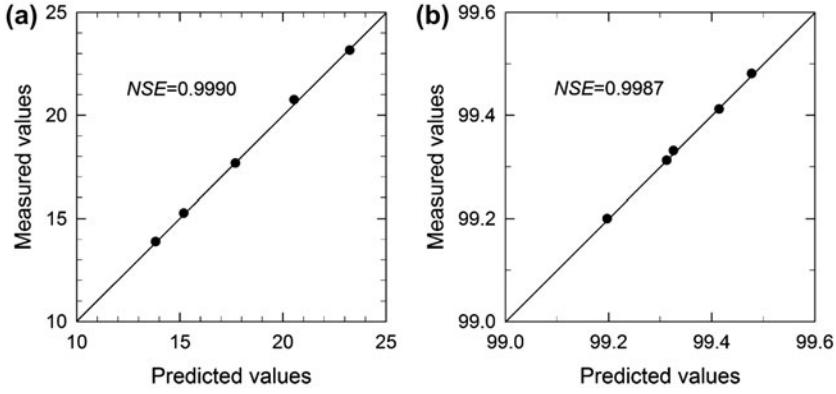

Fig. 4. Comparison of observed and predicated values for (a) the permeate recovery rate and (b) salt rejection rate of membrane. Individual points represent the values obtained under different conditions of the given system (see Section 3.1).

Table 1
Simulation results of flow rate and NaCl concentration at various monitoring points in the SWRO system (see Fig. 1) using two types of isobaric ERDs[a]

	Pressure exchanger		Dual work exchanger energy recovery	
Monitoring points	Flow rate (L/min)	NaCl concentration (mg/L)	Flow rate (L/min)	NaCl concentration (mg/L)
M1	15.0	33,720	15.0	33,720
M2	15.0	34,134	14.6	33,811
M3	30.0	33,921	29.6	33,759
M4	24.9	40,834	24.6	40,596
M5	24.9	40,529	25.0	40,169
M6	5.1	77	5.0	75
Feed pressure[b] (bar)	67.0		65.8	
Recovery rate (%)	16.9		16.4	

[a]Simulation is performed under 6% volumetric mixing rate and 0% overflush for PX and 1.5% volumetric mixing rate and 3% overflush for DWEER.
[b]Feed pressure and recovery rate represent the predicted values at monitoring points M3 and M6, respectively.

characteristics of both PX and DWEER to investigate their effects on the flow rate and salt concentration throughout various monitoring points M1–M6. Note that specific conditions were applied to the simulation as follows: c_{bulk} (the feed salt concentration) = 33,720 mg/L, u (the velocity of the flow channel) = 9.65×10^{-2} m/s (=30 L/min), p_f (the feed pressure) = 67 bar, and T (the feed temperature) = 293.15 K. As expected, the feed flow rate increased considerably at the monitoring point M3, where the raw feedwater and effluent from the isobaric ERD unit were joined, and decreased largely at the monitoring point M6, where the permeate was produced. Similarly, due to the combined effect of the volumetric mixing and overflush, the salinity level of the feed increased to a less extent at the monitoring points M2 and M3 and to a greater extent at the monitoring points M4 and M5 after passing through the isobaric ERD unit. From the table, it was determined that DWEER contributed to more flow rate reduction and less salinity level increase in the feed than PX at the monitoring points M2 and M3, although no significant difference was observed between PX and DWEER. The SWRO plant with PX showed slightly higher recovery rate (17.0%) and feed pressure (67.0 bar) as compared to those of DWEER (16.7% and 65.8 bar). Despite the same efficiency (95%) applied for both PX and DWEER, DWEER only caused the 1.3% (or 0.4 L/min) pressurized feed flow loss due mainly to the overflush, reducing the 1.8% feed pressure (or 1.2 bar) at M3 (data not shown). Collectively, the overflush is found to be more influential than the volumetric mixing at the pilot-scale plant, but those effects will be more pronounced in the SWRO

systems on medium and large scales, regardless of their relative contribution to the systems.

3.3. The impacts of membrane fouling

Membrane fouling which affects both the quantity and the quality of produced water gradually degrades the performance of the SWRO system over time [2]. So, this effect should be carefully addressed when assessing the dynamic behavior of membrane performance. Fig. 5(a) and (b) display the simulation results for the permeate recovery rate and salt concentration, respectively, using the transport equation in the RO membrane module which receives the updated resistance of the membrane from the fouling equation, Eq. (7), at each time step. In the figure, a comparison was made between the simulations under fouling (i.e. with declined flux across the membrane) and non-fouling conditions (i.e. without declined flux), during which any physical or chemical cleanings were not applied. It was shown from the figure that the permeate recovery rate and salt concentration varied considerably with respect to time due to the temporal changes in the raw feedwater quality. The recovery rate was significantly higher in a summer season than other seasons, which was likely attributed to the increased water permeability at higher water temperature as well as the decreased salt concentration due to the mixing of seawater with fresh water from rivers during a rainy season. However, the dilution effect had, in fact, a larger effect on the recovery rate than the temperature as no significant difference between the feedwater temperature in summer and autumn seasons was observed. The salt concentration of produced water increased as the membrane fouling was developed progressively over time (see Fig. 5(b)). The salt concentration was specifically high in an autumn season, showing a large difference between fouling and non-fouling conditions after the recovery rate declined significantly. In addition, although the predicted salt concentration was slightly lower in a winter season than the previous season regardless of the conditions, membrane fouling caused, on average, an increase in the salt concentration of produced water irreversibly. All these results indicated that our simulation reasonably described the temporal degradation of membrane performance in terms of the recovery rate and salt concentration based on the changes in the raw feedwater quality. The differences in the recovery rates between fouling and non-fouling conditions were 0, 13, 25, and 36% at 1, 90, 180, and 360 d, respectively. Their corresponding differences in salt concentrations recorded 0, 8, 17, and 21% at the selected time intervals. Note that the predicted recovery rate in the pilot-scale plant is much lower than that of the full scale SWRO system due to its small capacity of producing water daily (i.e. 14.8 m^3, see Section 2.1).

3.4. The impacts of feed pressure control

As membrane performance degraded over time, new control strategies such as the pressure control and membrane cleaning should be developed to maintain the target quantity (and quality) of produced water for the SWRO system. Among them, we applied the feed pressure control because this was easily implemented to the simulation. Note also that the pressure control can be done in both feed (p_f) and permeate sides (p_p), but the feed pressure control is preferred by industrial SWRO plants than the permeate side. Fig. 6(a) and (b) demonstrate the feasibility of

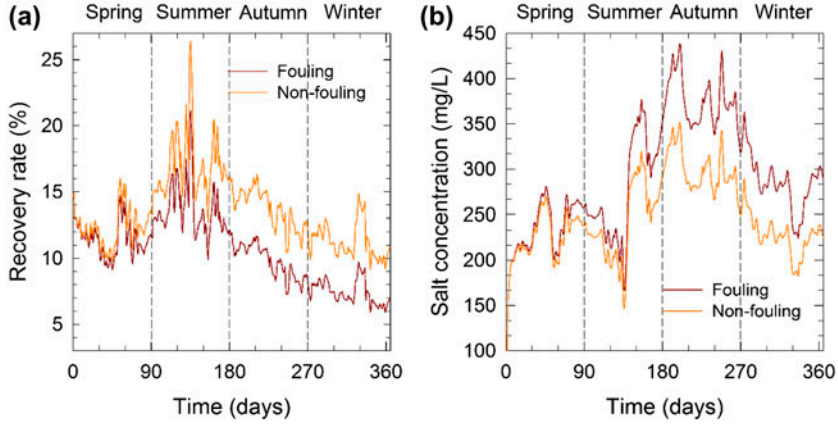

Fig. 5. Seasonal changes of (a) the recovery rate and (b) NaCl concentration of the permeate predicted under both fouling and non-fouling conditions for 2010. No cleaning condition was applied to the simulations.

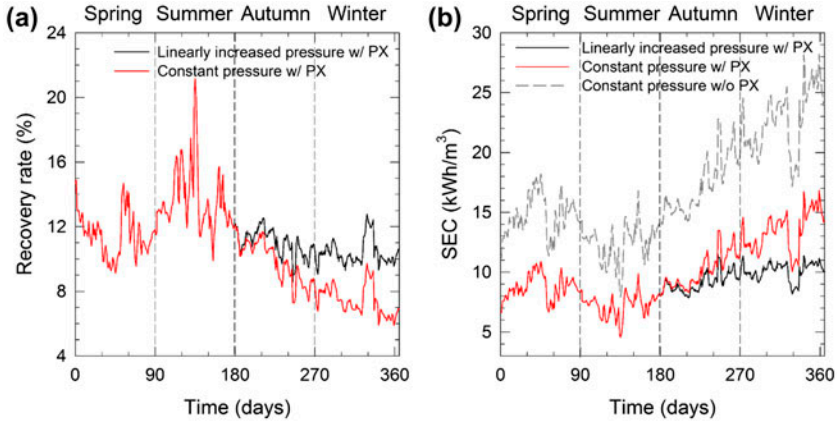

Fig. 6. Advantages of the linearly increased pressure of the feed flow in the given SWRO system in terms of (a) the recovery rate and (b) SEC, as compared to that of a constant pressure. The simulations are performed as the system performance progressively declined over time due to fouling, and the new control mode that increases the pressure of the feed flow linearly is applied after 180 d. In (b), PX out of two isobaric ERDs is used in the estimation of SEC.

the feed pressure control for the pilot-scale SWRO plant mounting PX in terms of the recovery rate and energy consumption, respectively. Here, we do not present the temporal changes in the permeate salt concentration because produced water already satisfies the target concentration level (<500 mg/L) typically accepted for the upper limit of drinking water, thereby the SWRO plant (see Fig. 5(b)). From Fig. 6(a), it was found that while the permeate recovery rate declined considerably due to the progressive development of membrane fouling, an increase in the feed pressure improved the recovery rate remarkably after 180 d. Note that membrane fouling causes a large deviation from the expected recovery rate and salt concentration from this period (see Fig. 5(a) and (b)). By increasing the feed pressure linearly from 55.2 to 66.5 bar, we were able to achieve the 3.7% improvement of the recovery rate at the end of the simulation.

Increasing the feed pressure may, however, lower the overall energy efficiency of the SWRO system while maintaining the amount of produced water. So, we investigated the energy efficiency of the pilot-scale plant in more detail in response to the pressure control and ERD–PX. Fig. 6(b) shows the temporal changes of SEC values (i.e. the energy consumed per unit cubic meter) in a year simulated under three different scenarios, i.e. a linearly increased pressure control with PX, constant pressure control with PX, and constant pressure control without PX. From the figure, the energy consumption for all scenarios was shown to increase towards the end of the simulation, but a large difference in SEC values between the scenarios mainly occurred after 180 d, as described in the recovery rate. Interestingly, the scenario that linearly increased the pressure control with PX consumed the lowest energy out of them, showing the benefits of the feed pressure control and ERD simultaneously. On average, the predicted energy consumption were 8.8 kWh/m^3 for the linearly increased pressure with PX, 9.9 kWh/m^3 for the constant pressure with PX, and 16.9 kWh/m^3 for one year for the constant pressure without PX. In other words, the use of PX in the pilot-scale plant saved the 41.4% of energy usage annually, and applying the feed pressure control on top of that achieved the 6.5% of additional energy saving. From these results, it is revealed that increasing the feed pressure improves both recovery rate and energy efficiency for the SWRO system at the pilot scale, and this effect will be truly remarkable with the help of the isobaric ERD.

4. Conclusions

The present work performs the simulation of the SWRO system at the pilot scale to identify the potential benefits of the isobaric ERD and feed pressure control against membrane fouling. PX, and DWEER were used to describe the overflush and mixing processes that affected the quantity and quality of the influent to the RO membrane module. In contrast, the feed pressure control was applied to assess the energy efficiency of the pilot-scale SWRO system while satisfying the target water quantity (and quality) under degradation conditions of membrane performance. The raw feedwater quality observed in seawater was also used to simulate those mechanisms under more realistic conditions at the pilot scale. The major conclusions can be summarized as follows:

(1) The feedwater quality for the SWRO plant varied considerably from season to season. Nonetheless, the transient model successfully simulated the permeate recovery and salt rejection rates at the pilot-scale plant under different feed concentrations (NSE = 0.9990 and 0.9987, respectively).
(2) Both PX and DWEER increased salt concentration slightly, whereas DWEER further reduced the feed flow rate than PX due to the volumetric flow loss of the pressurized feed. This, in turn, decreased the permeate recovery rate, requiring more feed pressure to increase the amount of produced water declined.
(3) A significant difference in the permeate recovery rate and salt concentration was observed between the simulations under fouling and non-fouling conditions. When membrane performance degraded progressively, an increase in the feed pressure not only recovered the permeate recovery rate, but also helped to save energy usage than the constant pressure control. The energy consumption was reduced further when the isobaric ERD was supported in the SWRO system.

Overall, this study proves the usefulness of the dynamic model at the pilot scale in developing efficient operation scenarios for the SWRO system in terms of energy use and water production.

Acknowledgments

This research was supported by the research project entitled "Smart Civil Infrastructure Research Program (grant number 14IFIP-C088924-01)" jointly funded by the Ministry of Land, Infrastructure and Transport in Korea (MOLIT) and Korea Agency for Infrastructure Technology Advancement (KAIA).

References

[1] L.F. Greenlee, D.F. Lawler, B.D. Freeman, B. Marrot, P. Moulin, Reverse osmosis desalination: Water sources, technology, and today's challenges, Water Res. 43 (2009) 2317–2348.
[2] C.Y. Tang, T. Chong, A.G. Fane, Colloidal interactions and fouling of NF and RO membranes: A review, Adv. Colloid Interface Sci. 164 (2011) 126–143.
[3] C. Fritzmann, J. Löwenberg, T. Wintgens, T. Melin, State-of-the-art of reverse osmosis desalination, Desalination 216 (2007) 1–76.
[4] R.L. Stover, Seawater reverse osmosis with isobaric energy recovery devices, Desalination 203 (2007) 168–175.
[5] T. Manth, M. Gabor, E. Oklejas, Minimizing RO energy consumption under variable conditions of operation, Desalination 157 (2003) 9–21.
[6] B. Schneider, Selection, operation and control of a work exchanger energy recovery system based on the Singapore project, Desalination 184 (2005) 197–210.
[7] R.L. Stover, Development of a fourth generation energy recovery device. A 'CTO's notebook', Desalination 165 (2004) 313–321.
[8] I.B. Cameron, R.B. Clemente, SWRO with ERI's PX Pressure Exchanger device—A global survey, Desalination 221 (2008) 136–142.
[9] G. Migliorini, E. Luzzo, Seawater reverse osmosis plant using the pressure exchanger for energy recovery: A calculation model, Desalination 165 (2004) 289–298.
[10] N. Park, B. Kwon, I.S. Kim, J. Cho, Biofouling potential of various NF membranes with respect to bacteria and their soluble microbial products (SMP): Characterizations, flux decline, and transport parameters, J. Membr. Sci. 258 (2005) 43–54.
[11] K. Spiegler, O. Kedem, Thermodynamics of hyperfiltration (reverse osmosis): Criteria for efficient membranes, Desalination 1 (1966) 311–326.
[12] M.Soltanieh, W.N.Gill', Review of reverse osmosis membranes and transport models, Chem. Eng. Commun. 12 (1981) 279–363.
[13] L. Song, S. Hong, J. Hu, S. Ong, W. Ng, Simulations of full-scale reverse osmosis membrane process, J. Environ. Eng. 128 (2002) 960–966.
[14] M. Mulder, Basic Principles of Membrane Technology, Springer Science & Business Media, Berlin, 1996.
[15] V. Gekas, B. Hallström, Mass transfer in the membrane concentration polarization layer under turbulent cross flow. I: Critical literature review and adaption of existing Sherwood correlations to membrane operations, J. Membr. Sci. 30 (1987) 153–170.
[16] K.L. Chen, L. Song, S.L. Ong, W.J. Ng, The development of membrane fouling in full-scale RO processes, J. Membr. Sci. 232 (2004) 63–72.
[17] A. Zhu, P.D. Christofides, Y. Cohen, Effect of thermodynamic restriction on energy cost optimization of RO membrane water desalination, Ind. Eng. Chem. Res. 48 (2008) 6010–6021.